UNIVERSIDAD
POLITECNICA
DE VALENCIA

cmt
motores térmicos

TRABAJO DE FIN DE MASTER

CONTRIBUCIÓN A LA REDUCCIÓN DE EMISIONES DE NOx EN MOTORES DIESEL SOBREALIMENTADOS MEDIANTE TÉCNICAS DE CONTROL PREDICTIVO

Realizado por: Pedro Cabrera López
Dirigido por: Carlos Guardiola García

Valencia, 18 de Octubre de 2010

Master en
Motores de Combustión Interna Alternativos

DEPARTAMENTO DE MÁQUINAS Y MOTORES TÉRMICOS

Introducción

El presente documento resume los trabajos realizados durante el periodo de docencia del Master en Motores de Combustión Interna Alternativos en el ámbito del modelado del motor diesel sobrealimentado y la implementación de un control para la reducción de contaminantes producidos por estos motores. En particular, se presta especial atención a la aplicación de controladores predictivos del tipo MPC (Model Predictive Control) para el control en bucle cerrado de las emisiones de NOx de tal forma que el controlador consiga, modificando diferentes parámetros del motor (acciones de control), que las emisiones de NOx sigan o alcancen una referencia marcada. De esta manera, es posible acotar las emisiones de NOx en transitorios del motor y por tanto, conseguir una reducción de los mismos en comparación al motor de serie sin la implementación del controlador mencionado.

El trabajo tiene como objetivo disminuir las emisiones de NOx producidas por los motores diesel actuales basándose en la capacidad que para ello tiene la mejora y la implementación de estrategias de control modernas. Para llevar a cabo dicho objetivo, se instala un sensor prototipo en el colector de escape del motor capaz de medir NOx de una manera rápida, se fijan unos parámetros claves que intervienen en la mayor o menor producción de emisiones de NOx, como son la tasa de EGR (exhaust gas recirculation) y el SOI (start of injection). Este trabajo mejora por lo tanto el resultado del sistema actual de control basado en el control del EGR, al permitir la modificación de las características de la inyección para mitigar los el efecto de los errores en el control de la tasa de EGR.
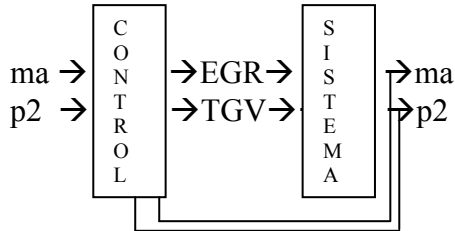
Para ello, una vez fijados los parámetros de actuación, es necesario centrarse en la obtención de modelos matemáticos en los que se refleja el comportamiento en la formación de dichas emisiones a la hora de variar estos parámetros. Una vez realizado esto, se implementa un controlador MPC y se realizan ensayos en el banco motor para observar el comportamiento del motor y de las emisiones de NOx con el controlador MPC funcionando. Se debe conseguir una mejora en las emisiones de NOx a través de la obtención y estudio de unos modelos robustos y un controlador que sea rápido y que tenga en cuenta la medida de emisiones de NOx.

Antecedentes

El trabajo realizado se enmarca en el control de emisiones contaminantes a través de la implantación de nuevos sensores y la implementación de algoritmos de tipo MPC. Para mostrar más clara la aproximación metodológica y los antecendentes se muestra el esquema que se explica a continuación.

UNIVERSIDAD POLITECNICA DE VALENCIA

cmt motores térmicos

TESIS José Vte. Ortiz

ma →
p2 →
CONTROL
→ EGR →
→ TGV →
SISTEMA
→ ma
→ p2

Del Re, Glielmo, Guardiola and Kolmanovsky (Eds.) Automotive Model Predictive Control: Models, Methods and Applications

Summer School on Automotive Model Predictive Control

INCLUSIÓN DE NUEVOS SENSORES

- Sensor NOx
- Sensor caudal EGR
- Sensor O2

TÉCNICAS DE BY-PASS

- Bypass sobre SOI
- Bypass sobre EGR
- Bypass sobre WG/TGV
- Bypass sobre mf, ...

DIFERENTE ARQUITECTURA

- HP→ EGR en alta presión
- LP→ EGR en baja presión →
→ comportamiento más lineal →
→ mejora de cara al control MPC

MÉTODOS DE CONTROL

- Modelo MIMO
- Quadratic Programming MPC
- Restricciones
- Modelos no lineales (H-W models)

EGR HP-LP
- Control con el conjunto {ma, O2, p2}
- Actuación {EGR, TGV}

INCLUSIÓN SENSOR NOx
- Control con el conjunto {ma, NOx, p2}
- Actuación {EGR, SOI, TGV}

INCLUSIÓN SENSOR HUMOS y PAR
- Control {NOx, Humos, Par}
- Actuación {EGR, SOI, TGV, mf}

TESIS

El trabajo continúa la línea iniciada en el instituto CMT-Motores Térmicos por la tesis de José Vicente García Ortiz. "*Aportación a la mejora del control de la gestión del aire en motores Diesel turboalimentados mediante distintos algoritmos de control*" en la cual se implementa un algoritmo para el control en bucle cerrado del gasto de aire en la admisión y de la presión de sobrealimentación ajustando la posición de la válvula de EGR y la posición de la TGV en un motor diesel sobrealimentado moderno. Por otra parte, el autor del presente trabajo ha realizado una estancia formativa en la Johannes Keppler Universitat de Linz sobre *Automotive Model Predictive Control*, y ha realizado una labor de documentación en lo relativo al estado del arte sobre la materia (consultar por ejemplo *Automotive Model Predictive Control: Models, Methods and Applications*).

Aportaciones

El carácter diferenciador del presente trabajo se basa en cuatro aspectos:

- La utilización de nuevos sensores existentes orientados a control, como los sensores de NOx, de concentración de O2, de gasto de EGR, etc.

- La utilización de técnicas de bypass, que permiten la modificación en tiempo real de las acciones de control (permitiendo el control conjunto del aire y la inyección) y la implementación de controladores mediante técnicas de prototipado rápido.

- La aplicación a motores con diferentes arquitecturas (EGR alta presión y baja presión, sistemas de sobrealimentación secuenciales, etc.)

- La aplicación de técnicas de control, modelo e identificación (MPC lineales con restricciones, optimizadores basados en *quadratic programming*, modelos Hammerstein-Wiener, etc.)

Aunque el desarrollo independiente de cada uno de estos factores excede el objetivo de los trabajos planteados, la combinación de estos elementos permite asegurar su carácter innovador.

Trabajos realizados y resultados

Dentro de la línea de trabajo presentada se han realizado varios trabajos de los cuales, por su relevancia, se resaltarán dos. Ambos trabajos han permitido la redacción de artículos que se adjuntan como anexos al siguiente documento.

En el **artículo 1, "*Considerations on the low pressure EGR system control in turbocharged diesel engines*"** (**ANEXO 1)**, que será enviado a *IEEE Transactions on Control System Technology*, se realiza un estudio de las particularidades de control de un sistema de EGR de baja presión y se compara con el sistema habitual de alta presión. En este trabajo se realiza una primera aplicación de las técnicas de modelado y control multivariable MPC para el control del sistema de renovación de la carga empleando

sensores convencionales o no (como la medida de la concentración de O2 en el colector de admisión). Dicho trabajo básico se une a otros, no reportados, donde se ha estudiado el empleo de otros sensores alternativos (gasto de EGR, O2 escape, etc.). Aunque en dicho trabajo aún no se plantea un control en bucle cerrado sobre los contaminantes, se estudia la controlabilidad y la selección de sensores para el control del sistema de renovación de la carga.

Paralelamente a lo anterior, se desarrolla un sistema de bypass que permite comunicarse y transferir valores de variables desde y hacia la ECU, de tal forma que se pone en marcha una plataforma de adquisición y registro de datos en tiempo real que se enlaza con el sistema de bypass, permitiendo el envío y recepción de datos entre el binomio motor-sistema en tiempo real. Con la puesta en marcha de dicho sistema se estudia y se realiza la implementación de métodos de control con algoritmos cuadráticos, centrándose en el controlador predictivo basado en modelos (MPC) con restricciones pudiendo así tener la posibilidad de actuar de manera controlada sobre las variables del motor posición de EGR y SOI.

Posteriormente y siguiendo esta línea de investigación, se instala un sensor de NOx en el escape, se realizan ensayos en banco motor utilizando señales estímulo actuando sobre EGR y SOI registrando estos valores y la respuesta del motor registrando los valores de respuesta referentes a NOx y gasto de aire (ma). Además, se registra el par y la opacidad de los gases de escape a través de la instalación de un opacímetro teniendo así información acerca de los humos emitidos. Se obtienen modelos matemáticos lineales a través de procesos de identificación y se genera a partir de estos modelos un controlador MPC en bucle cerrado que permite acotar y seguir una referencia de NOx dada a la vez que sigue una referencia con escalones de gasto de aire. Se describe este trabajo en el **artículo 2** *"NOx closed-loop control in a turbocharged diesel engine through injection and air path coordinated model-based control"*, adjunto como **ANEXO 2**, que será enviado a *Control Engineering Practice*.

En él, se demuestra la posibilidad real de controlar los NOx en bucle cerrado. Además se muestra que es posible mitigar la emisión de NOx durante los transitorios en el sistema de EGR o sobrealimentación. Para ello se ha empleado una corrección rápida del SOI. Esto puede hacerse en bucle cerrado (si existe un sensor de NOx) o abierto (sin sensor).

En la actualidad se continúa el trabajo estudiando e incorporando al control el par motor y los humos, considerando además el gasto de fuel como perturbación y como elemento adicional a controlar para conseguir avances en los resultados de la reducción de emisiones. Además se pretende mejorar el sistema de control mediante el empleo de modelos matemáticos no lineales basados en técnicas como Hammerstein-Wiener para mayores rangos de funcionamiento del motor, lo que permitirá un control preciso durante los transitorios de carga y régimen. El desarrollo de estos trabajos será el objetivo de la *tesis doctoral* en la que se enmarcan los trabajos presentados.

ANEXO 1

1

Considerations on the low pressure EGR system control in turbocharged diesel engines

José Manuel Luján, Carlos Guardiola, Benjamím Pla and Pedro Cabrera

Abstract— Although high pressure exhaust gas recirculation has been commonly used in turbocharged diesel engines for controlling the NOx formation, recent advances in after-treatment and material technology make possible using a low pressure architecture, which recirculates the exhaust gas upstream the compressor. The paper presents a basic study of control aspect related to the low pressure architecture, emphasising the similarities and differences with the high pressure system. Data coming from experimental tests with both configurations, and from a one-dimensional wave action model simulations, are combined for the analysis of the input-output paring, linearity and the transient performance of both systems.

Index Terms— Diesel engine, engine control, exhaust gas recirculation, turbocharging, model predictive control.

I. INTRODUCTION

EXHAUST gas recirculation (EGR) has become a widespread technique for controlling nitrogen oxides (NOx) formation and emission in current automotive turbocharged diesel engines [1], [2]. Although low pressure (LP) EGR (Figure 1, top) is not a new technical solution has been known for long [3], it was discarded because compressor wheel damaging and soiling and acid corrosion problems in the intercooler [4]. Hence, high pressure (HP) EGR system (Figure 1, bottom) is now the standard solution. However, new engine technologies, like particulate filters for exhaust gas after-treatment [5], the development of high resistance intercoolers [6] and the generalization of low sulfur content fuels, could allow using low pressure EGR system.

Despite HP-EGR system control has been a major topic of research because it is strongly coupled with the turbocharging system [7], [8], there is little knowledge about LP-EGR control. This paper compares the two systems and analyses the advantages and disadvantages of the LP-EGR system from the control point of view. For the present study, simulation results from a one dimensional engine simulation code and experimental results are combined.

II. ENGINE MODEL AND EXPERIMENTAL FACILITY

The engine used for the study is a 2-litre 4-cylinder turbocharged diesel engine whose main characteristics are provided in Table I. The series engine has a variable geometry turbine (VGT) for boost pressure control and a HP-EGR with a electrically piloted valve for the EGR rate control. For the present work, an auxiliary LP-EGR system and a water cooled intercooler were installed as sketched in Figure 2. A back

J.M. Luján, C. Guardiola, Benjamín Pla and Pedro Cabrera are with the CMT-Motores Térmicos at the Universidad Politécnica de Valencia.
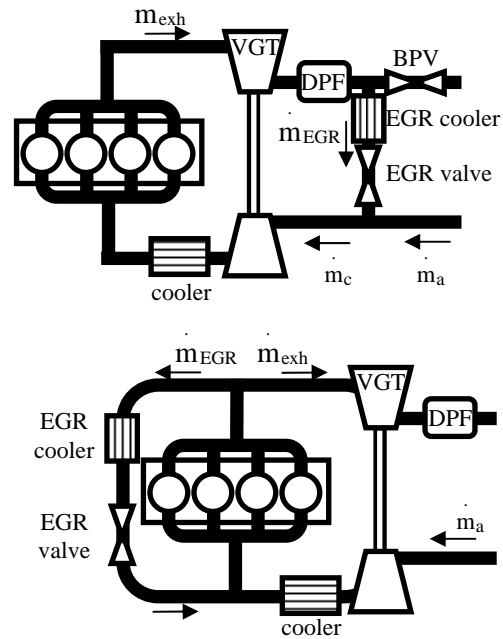

Fig. 1.　Schema of the HP-EGR (top) and LP-EGR configurations.

TABLE I
ENGINE MAIN CHARACTERISTICS.

Displacement	1998 cm^3
Bore x Stroke	85 x 88 mm
Valves	4 / cylinder
Compession ratio	18:1
Turbocharger	Garret VNT GT 1749V
After-treatment	Oxi-catalyst + DPF
Max. power / speed	100 kW / 4000 rpm
Max. torque / speed	320 Nm / 1750 rpm

pressure valve (BPV) was used for increasing the pressure drop in the exhaust system, thus increasing the EGR rate in the cases when EGR valve was fully open but pressure gradient was not sufficient.

An external control system was used for controlling EGR valves and VGT, while the engine was instrumented for the paper purposes with an intake manifold pressure sensor, two hot wire anemometers (upstream and downstream the LP-EGR junction) and a broadband lambda sensor for intake manifold gas composition determination. This last sensor was included because recent works suggest it to be an advantageous alternative for controlling NOx formation with respect to the classical approach of controlling air mass flow [9], [10].
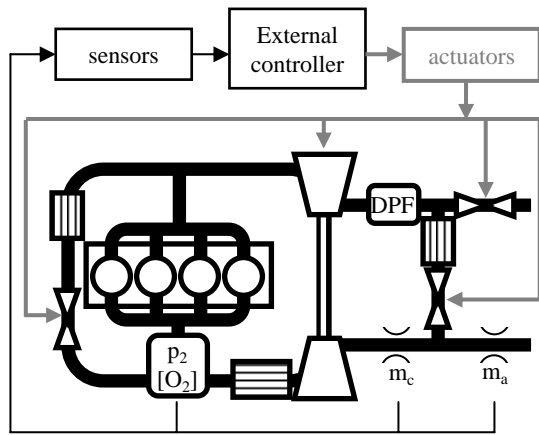
Fig. 2.　Lay-out of the experimental facility.

Additionally to the experimental facility, a wave action model [11] one dimensional code was used for simulating the engine operation. Specific sub-models are used for the turbocharger and the combustion process [12]. Finally the model is linked with Matlab for control system simulation and evaluation. Engine model was adjusted using geometrical engine parameters and specific engine tests. Because of the physical approach used in the fluid dynamics model, the model is able to properly describe the instantaneous evolution (including in-cycle pulsation) of gas temperature, speed, composition and pressure at any point of the engine air-path.

III. STATIC GAIN ANALYSIS

In the classical HP-EGR architecture, the coordination of the VGT and EGR actions to allow an optimal engine performance is a challenging task due to the strong coupling between the two systems. For investigating this aspect, a set of simulations of steady conditions with constant injected fuel mass quantity and engine speed, and different EGR valve and VGT positions were performed. The simulations were also replied in the LP-EGR configuration.

Maps in Figure 3 summarise the result of these simulations, where the steady interactions between the VGT and EGR systems and their effects on air mass flow (m_a), intake pressure (p_2) and intake burnt gas fraction (BGF) are shown. The upper row of Figure 3 contains the static maps of air mass flow as a function of VGT and EGR positions for the two studied EGR architectures. When the HP-EGR valve remains closed, the air mass flow through the engine increases as the VGT closes. However, when the HP-EGR valve is open, the opposite trend is observed. To close the VGT vanes leads to an increase in the exhaust pressure. If the HP-EGR valve is closed, the whole exhaust mass flow will go through the turbine, accelerating the turbocharger and increasing the mass flow through the compressor. Nevertheless, as the EGR valve gets open the increase in exhaust pressure also leads to an increase in the recirculated flow, then reducing the air mass flow. Both effects, which are opposite, provide a gain inversion in the relation between air mass flow and VGT position. The operating conditions at which this gain inversion appears

depend on the EGR valve position, and also on other engine parameters such as the engine speed and fuelling rate.

The central row of Figure 3 shows the static maps of intake pressure as a function of VGT and EGR positions for both EGR systems. Since the exhaust gas recirculation does not reduce the energy availability at the turbine inlet when the LP-EGR is employed, the intake pressures achieved when the LP-EGR valve is open becomes higher than those obtained when the HP-EGR valve is open. In fact, from the orientation of the lines of constant intake pressure it can be stated that the intake pressure is almost independent of the LP-EGR valve opening. This aspect and others related to the signal pairing will be treated in section III-A.

Finally, at the bottom part of Figure 3 the static maps of intake burnt gas fraction as a function of VGT and EGR positions are shown. In this case, it can be observed how the burnt gas fraction of the intake gases is independent of the VGT position when the LP-EGR architecture is employed. On the contrary, the VGT position increases its impact on the exhaust gas recirculation as the HP-EGR valve gets open. In addition, figure 3 shows that the LP-EGR system does not allow to achieve EGR rates as high as those obtained with the HP-EGR architecture, pointing out the requirement of a BPV placed downstream the EGR extraction in order to increase the pressure difference between exhaust and intake lines, thus allowing higher EGR rates.

Results shown in figure 3 suggest that the LP-EGR architecture is essentially decoupled if boost pressure and BGF (or oxygen concentration) are considered. With regards to the traditional approach, where air mass flow and boost pressure are used as controlled variables in the HP-EGR, this can be considered a clear advantage.

Another important issue is related to the ability of the LP-EGR system of feeding an homogeneous mix of fresh air and gas burnt. Although this can not be checked through the one dimensional code, since it does not consider the three dimensional distribution of the gas composition, computational fluid dynamics and experimental [13] results reveal that the HP-EGR design can importantly impact on the homogeneity of the gas mix.

For the tested engine, an experiment consisting on using eight alternative probes for feeding a NDIR gas analyzer was done, which determined CO_2 concentration, which is proportional to the BGF. A steady operation point was tested, and independent measurements for each one of the probes were obtained. Top plot in Figure 4 illustrates the huge dispersion obtained at the different locations of the intake manifold. On the other hand, if the engine was operated with the LP-EGR architectiture, all probes provide an equivalent measurement, as shown in bottom plot in Figure 4.

This lack of homogeneity in the HP-EGR configuration can have important effects on the engine operation. On one hand, the non homogeneity can imply that each individual cylinder has different gas composition, which could impact on the engine out emissions, and even in the stability of the combustion if low temperature combustion (LTC) methods are used [14]. On the other hand, this fact implies a great difficulty for the implantation of intake gas composition sensors (as
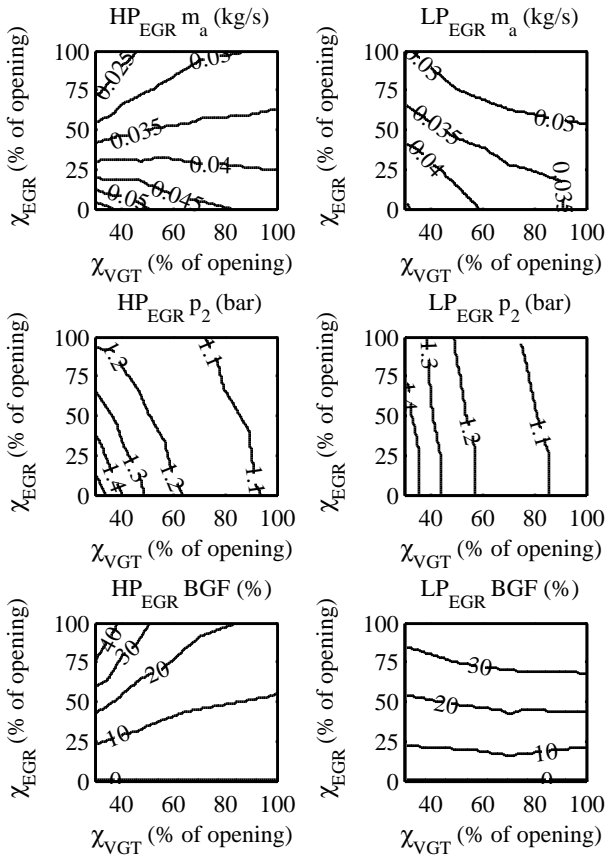
Fig. 3. Map of m_a, p_2 and BGF when varying EGR and VGT positions for the HP-EGR system (left) and the LP-EGR system (right). Obtained from the engine model at 2400 rpm and 20 mg/str.

Fig. 4. Distribution of the CO_2 concentration in 8 different probes at the intake manifold for the HP-EGR system (top) and the LP-EGR system (bottom) in steady operation.

broadband lambda sensors): the measurement provided by the sensor can be not representative of the mean BGF. Correcting the deviation of the sensor is not straightforward as it varies in a non-linear way. Furthermore, the homogeneity is strongly dependent on the operating conditions, since the wave pattern established in the manifold is critically affected by the engine speed, and also by the recirculated burnt gas fraction.

In opposition, LP-EGR architecture is not affected by these effects: the long path used along the intake system (including the pass through the compressor) ensures an homogeneous composition of the gas mix. Hence, all cylinders have the same admitted gas composition, and its value can be easily determined through a sensor in the intake manifold. The LP-EGR long path also ensures a proper refrigeration of the gas mix, since it passes through the intercooler (while EGR cooler is still needed for avoiding excessive temperature in the intake mix and protecting all elements along the line).

Despite of all these advantages in the static performance of the LP-EGR system, the long path used can negatively impact the system dynamic response. In addition, the additional BPV needed in some situations for increasing the pressure drop at the exhaust system (specially at low engine speed) complicates the air path control.
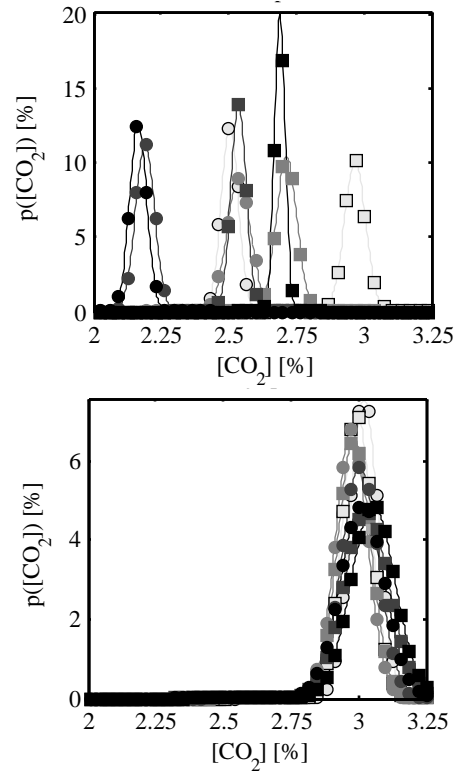
A. Signal pairing

On the basis of the static gain maps shown in Figure 3, and using the method proposed by Bristol [15], it is possible to study the convenience of a given input-output pairing. The method is based on studying the coefficients μ_{ij} obtained through the input-output gain matrix Φ, where

$$\mu_{ij} = \Phi_{ij} \left(\Phi^{-1} \right)_{ji} \qquad (1)$$

μ_{ij} determines the coupling between input i and output j. $\mu_{ij} = 0$ implies that the given input does not influence the output, while $\mu_{ij} > 0$ marks the relative influence of the input on the output; $\mu_{ij} < 0$ is associated with instabilities in the control. Since due to the construction of the coefficients $\sum_j \mu_{ij} = 1$, perfect decoupled system occurs with a given $\mu_{ij} = 1$ while the rest of coefficients for the same output are equal to 0. In the case of a 2×2 system, it is evident that $\mu_{11} = \mu_{22}$ and $\mu_{12} = \mu_{21}$.

For the studied system, three different sets of outputs can be selected: $\{m_a, p_2\}$, $\{BGF, p_2\}$ and $\{m_a, BGF\}$. For each one of the sets and each EGR configuration, maps representing the value of μ_{11} and μ_{12} at the studied operation condition (2400 rpm, 20 mg/str) in the whole range of regulation of the VGT and EGR valve can be built. The variation of these coefficients can be used for inferring the effect of the EGR and VGT positions on the system controllability.

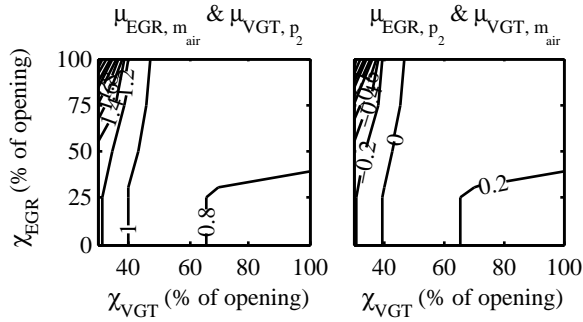Figures 5 and 6 show the μ_{ij} maps for the $\{m_a, p_2\}$ set, in HP- and LP-EGR configurations respectively. The maps

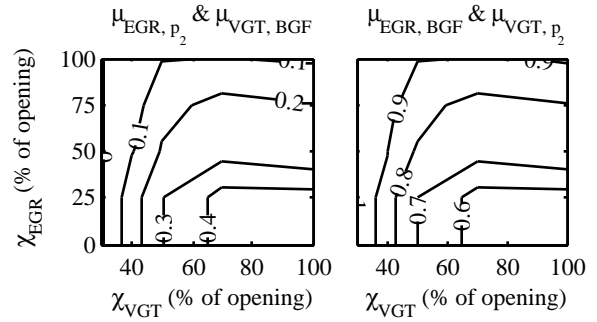Fig. 5. Maps of μ values in the HP-EGR configuration considering $\{m_a, p_2\}$ set at 2400 rpm and 20 mg/str.

Fig. 7. Maps of μ values in the HP-EGR configuration considering $\{BGF, p_2\}$ set at 2400 rpm and 20 mg/str.

Fig. 6. Maps of μ values in the LP-EGR configuration considering $\{m_a, p_2\}$ set at 2400 rpm and 20 mg/str.

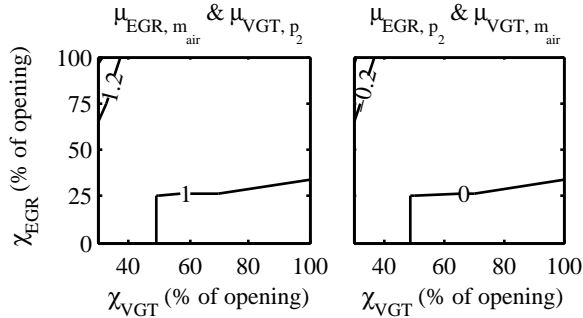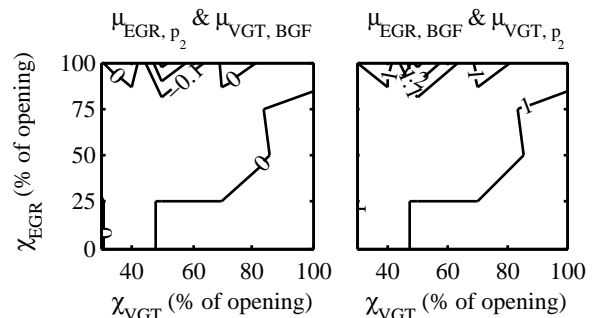Fig. 8. Maps of μ values in the LP-EGR configuration considering $\{BGF, p_2\}$ set at 2400 rpm and 20 mg/str.

obtained for the HP-EGR system confirm the convenience of the usual pairing (m_a-EGR and p_2-VGT) but they remark that in the case of the VGT very closed, the risk of instabilities exists if both signals are controlled simultaneously. In the case of the LP-EGR system, this issue is less evident, and a perfect decoupled system occurs for most of the EGR-VGT range.

In case that $\{BGF, p_2\}$ is selected as output pair, the maps of Figures 7 and 8 are obtained. In this case the system is not decoupled for the HP-EGR architecture, although instabilities do not occur. Note that the coupling of the system increases for very open positions of the VGT, since then the sensitivity of the ssytem to the EGR valve position is lower. Although it is possible to control the system, multivariable control techniques will be necessary due to the important crossed influence. The suggested pairing for this system is BGF-EGR and p_2-VGT. On the other hand, the LP-EGR system presents an almost decoupled situation, where VGT can be used for controlling p_2 and EGR for BGF.

Finally, maps for the $\{m_a, BGF\}$ set (not shown) reveal instabilities for both the LP-EGR and HP-EGR cases. This is due to the fact that the EGR position has an important direct influence on both quantities, which are importantly correlated. Hence these to variables must be rejected as control pairs.

IV. DYNAMIC ANALYSIS

For the analysis of the dynamic response of the system, different simulations with the wave action model were done. In the initial simulations engine speed and injected fuel mass was

kept constant, and step transitions were applied to the EGR and VGT (additionally the effect of the BPV was checked for the LP-EGR system). Results on the evolution of the main variables are shown in Figure 9.

Results for a step in the VGT position are shown in left-hand plots. Results are presented for the HP-EGR system (grey) and the LP-EGR system (black) and two different operating conditions: closed EGR valve (dotted), and partially open EGR valve (full). Two remarkable effects can be noticed in line with the conclusions of the steady analysis: in LP-EGR configuration VGT do not significantly influences the BGF, and the sign of the variation on m_a on the HP-EGR system when a step in the VGT is applied depends on the EGR position. Both issues confirm that the LP-EGR system is more easily decoupled than the HP-EGR system. Concerning the dynamics of the response in m_a and p_2, no significant differences are noticed between both architectures.

When considering the response to variations in the EGR position (central plots) a significant drawback of the LP-EGR system can be highlighted: there is a huge delay (up to 0.3 s) between the EGR step occurrence and the variation of the BGF in the intake manifold. This delay is attributed to long line between the EGR junction and the intake manifold (dotted line represents the BGF just downstream the junction, which reacts similarly to the HP-EGR system). This delay can compromise the performance of the engine during load steps, as will be discussed later on.

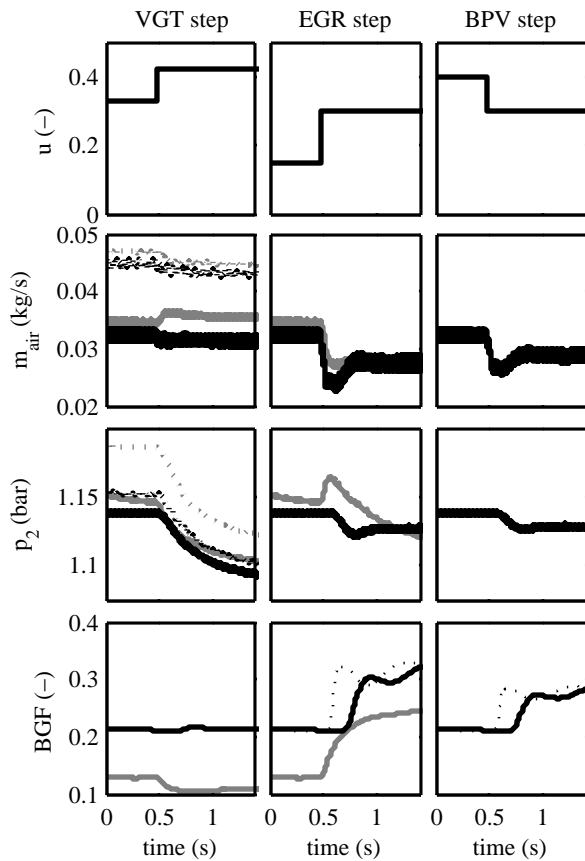Another significant difference is that the LP-EGR system

Fig. 9. Results of the HP-EGR system (—) and the LP-EGR system (—) for steps in the different control variables. Left: step in VGT position, for partially open EGR (full) and closed EGR (broken). Centre: step in EGR position (dashed: BGF downstream the EGR junction). Right: step in BPV position (dashed: BGF downstream the EGR junction).

TABLE II

SIMULATIONS.

	1200 rpm	2400 rpm
10 mg/str	A	B
20 mg/str	C	D

avoid the non-minimum phase response that can appear in the HP configuration on the boost pressure (which results from the opposed effects of the fast pressure equalisation in the manifolds and the slow turbocharger dynamics).

Finally, LP-EGR system allows the control of the EGR rate through the BPV. The effect of this valve (shown on right-hand plots in Figure 9) is similar to that of the EGR valve. However, it impacts the engine efficiency since it increases the backpressure at the exhaust manifold, and thus it is only foreseen for increasing the EGR rate once EGR valve becomes saturated.

A second study was done simulating a pseudo-random binary sequence in both EGR and VGT in 4 different operating conditions, which are summarised in Table II. The results of such tests for the HP- and LP-EGR systems are shown in Figure 10. In both systems important differences in the gain of the system are noticed depending on the considered operating conditions. This has a significant impact on the control system,
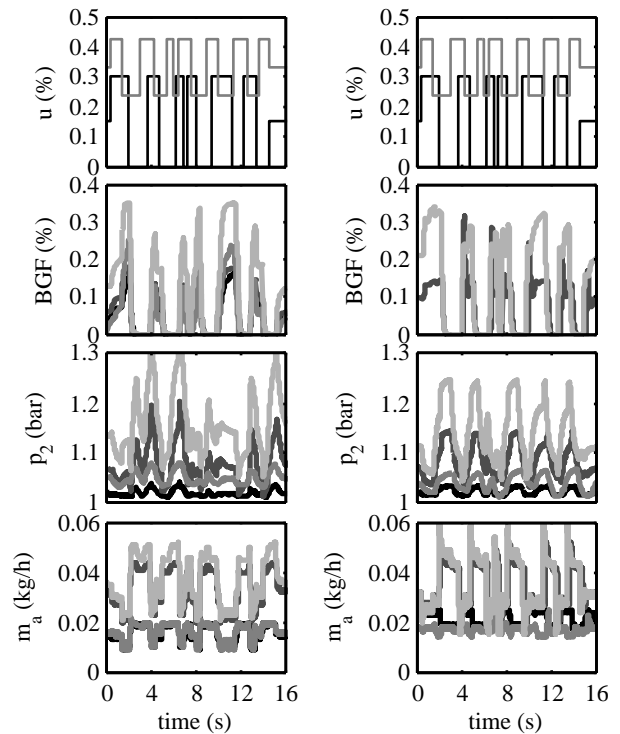

Fig. 10. Evolution of BGF, p_2 and m_a for a pseudo-random binary sequence in VGT and EGR positions in conditions A to D (black to light grey). Left: HP-EGR; right: LP-EGR.

since controller parameters must be scheduled in order to be adapted to the engine operating conditions.

Same general trends in the gain are observed for the two cases: the influence of the VGT and EGR variations is increased in the cases with higher exhaust energy availability (i.e. higher injected fuel mass). However, for a given operating condition (i.e. constant engine speed and injected fuel mass), LP-EGR presents a quasi-linear behaviour, while this is not the case of the HP-EGR system due to the sign inversions that were discussed in the previous section.

For illustrating this issue, Figure 11 shows the results of a linear identification of the system for the HP-EGR (left) and LP-EGR (right) systems for case D. In order to cope with the nonlinearity of the gain, a static non-linear transformation of the input quantities (EGR and VGT positions) was performed beforehand, hence resulting in a Hammerstein model.

Identified model for the LP-EGR can properly predict system response, while HP-EGR system model fail in some situations (squared region in right plot of Figure 11). Hence, model based control [16] techniques can be more easily applied to the LP-EGR system than in the HP-EGR case. In order to mitigate this aspect, some researches suggest using different controllers depending on the EGR valve position [9], thus adding a third scheduling variable beyond engine speed and load.

Finally, the effect of load transients was studied. Experiments on the engine were used for that, and those experiments served as input data for the simulations. Figure 12 presents the results of such experiment in the LP- and HP-EGR
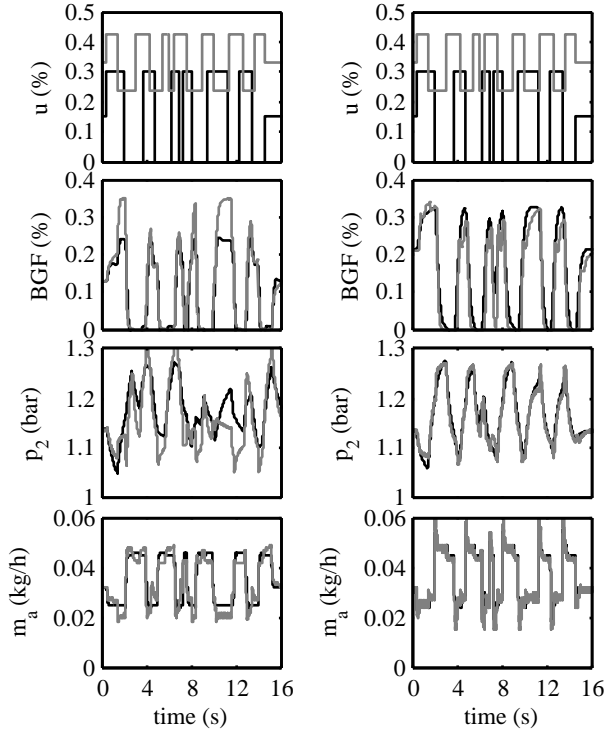
Fig. 11. Hammerstein model identified (—) compared with wave action model results (—) at operating conditions D. Left: HP-EGR; right: LP-EGR.
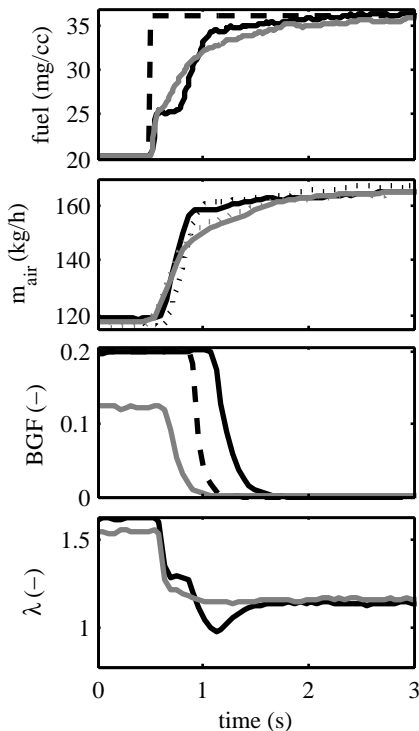

Fig. 12. Evolution during a load response for the HP-EGR system (—) and the LP-EGR system (—). Dotted lines in the m_a plot correspond to experimental values.

configurations. Due to the control system configuration in the series ECU, the EGR valve was directly closed when the load step request occurred (because it is an air deficient situation); on the other hand, the intake pressure is controlled in open loop with the VGT opening. In this sense, the VGT described the same trajectory during the load transient regardless the EGR loop employed. As far as the EGR opening does not reduce the available energy to drive the turbine when the LP-EGR architecture is employed, at the starting conditions of the transient the turbocharger speed is higher with the LP-EGR loop, which allows a faster air mass flow rise during the load step. The smoke abatement strategy of the standard ECU was based on the air mass flow measurement. According to the air mass flow measurement, the fuel mass flow in the test with the HP-EGR architecture was reduced to avoid a poor air-to-fuel ratio that could produce smoke spikes. Regarding the LP-EGR test the faster air mass flow response allowed a higher injection rate. Nevertheless, in the case of the LP-EGR system a significant delay exists between the closing of the EGR valve and the variation of the BGF in the intake manifold;then a significant overshoot appeared in the air-to-fuel ratio which for sure leaded to a significant smoke peak. In order to avoid that, it is necessary to completely redefine the fuel limiter calibration for the LP-EGR system, which impacts the engine load response.

V. CONCLUSIONS

The present paper shows a comparison between HP- and LP-EGR architectures from the point of view of engine control. A set of experimental and modelling studies have been carried out to reach the following conclusions:

- The static gain analysis has shown that with the LP-EGR system the BGF is decoupled from the VGT opening; similarly, the intake pressure is almost independent of the EGR valve opening. On the contrary, a strong coupling between the previous signals is observed with the HP-EGR architecture. Regarding the air mass flow, a gain inversion has been observed with the HP-EGR loop, since the VGT closing leads to an air mass flow increase when the EGR valve is closed, but an air mass flow decrease when the EGR valve is large open. This behaviour has not been observed with the LP-EGR architecture.

- From the static gain analysis, a study of the signal pairing for air management control has been carried out. The main conclusion is that the coupling between EGR and VGT with the HP-EGR layout make air path control tasks difficult: when the standard control pair $\{m_a, p_2\}$ is chosen there is a risk of instability when the VGT is closed and a simultaneous control of both variables is required; if the control pair $\{p_2, BGF\}$ is selected, the system will be stable, but strongly coupled. On the contrary, with the LP-EGR architectures the air path can be more easily controlled with both $\{m_a, p_2\}$ and $\{p_2, BGF\}$. Particularlly, the control set $\{p_2, BGF\}$ is specially suitable for the LP-EGR loop since the BGF does not depend on the VGT opening, and the EGR valve hardly affects intake pressure. As far as the control pair

$\{m_a, BGF\}$ is concerned, the engine behaviour with this control set is unstable regardless the EGR loop employed due to the strong effect of the EGR opening on both control variables.

- The long path followed by the gas from the air-EGR junction to the cylinders allows a perfect mixing between this two species; then a broadband lambda sensor placed anywhere in the intake manifold provides a representative value of the intake O_2 concentration. On the contrary, the non homogeneity in the intake charge when HP-EGR configurations are used prevents lambda sensor measurement from being representative of the real cylinder intake O_2 concentration, which involves difficulties when this sort of sensors are used with control purposes.

- The dynamic analysis has confirmed the conclusions obtained from the static maps presented, and also has shown the non-minimum phase behavior of the p_2 with the EGR opening when the HP-EGR configuration is used. In addition, from the dynamic analysis the important BGF delay with the LP-EGR loop can be observed. This delay is due to the high distance between the air-EGR junction and the cylinders.

- The modeling of pseudo-random binary evolutions for both EGR and VGT positions at different engine conditions has allowed to conclude that while the LP-EGR loop shows a quasi-linear behaviour, the HP-EGR architecture involves important non-linearities that restrict the linear identification to local regions.

- The analysis of the engine evolution during a load transient has shown that despite of the faster air mass flow evolution with the LP-EGR architecture, the BGF delay prevents the air to fuel ratio to keep above the minimum limits, which involve important smoke emissions. In this sense, an adaptation of the fuel limiter calibration will be required if the LP-EGR architecture is employed.

REFERENCES

[1] N. Ladommatos, S. Abdelhalim, and H. Zhao, "The effects of exhaust gas recirculation on diesel combustion and emissions," *International Journal of Engine Research*, vol. 1, pp. 107–126, 1999.

[2] M. Lapuerta, J. Hernández, and F. Gimenez, "Evaluation of exhaust gas recirculation as a technique for reducind diesel engine nox emissions," *Proc. Inst. Mech. Eng. Part D-J. Automob. Eng.*, vol. 214, pp. 85–93, 2000.

[3] R. Baert, D. Beckman, and A. Veen, "Efficient egr technology for future hd diesel engine emission targets," *SAE paper 1999-01-0837*, 1999.

[4] S. Moroz, G. Bourgoin, J. Luján, and B. Pla, "A 2.0 litre diesel engine with low pressure exhaust gas recirculation and advanced cooling system," *The Diesel Engine Conference, Proceedings of the SIA 2008 Conference, Rouen, France*, 2008.

[5] A. Walker, "Controlling particulate emissions from diesel vehicles," *Topics in Catalysis*, vol. 28, pp. 165–170, 2004.

[6] U. Krger, S. Edwards, E. Pantow, R. Lutz, R. Dreisbach, and M. Glensvig, "High performance cooling and egr systems as a contribution to meeting future emission standards," *SAE paper 2008-01-1199*, 2008.

[7] M. van Nieuwstadt, I. Kolmanovsky, P. Moraal, A. Stefanopoulou, and M. Jankovic, "Egr-vgt control schemes: Experimental comparison for a high-speed diesel engine," *IEEE Control Systems Magazine*, vol. 20, pp. 63–79, 2000.

[8] A. Stefanopoulou, I. Kolmanovsky, and J. Freudenberg, "Control of variable geometry turbocharged diesel engines for reduced emissions," *IEEE Trans. on Cont. Sist. Technol.*, vol. 8, pp. 733–745, 2000.

[9] P. Langthaler and L. Del Re, "Fast predictive oxygen charge control of a diesel engine," *Proceedings of the American Control Conference*, pp. 4388–4393, 2007.

[10] J. Arrègle, J. López, C. Guardiola, and C. Monin, "Sensitivity study of a nox estimation model for on-board applications," *SAE paper 2008-01-0640*, 2008.

[11] J. Galindo, J. Serrano, F. Arnau, and P. Piqueras, "Description and analysis of a one-dimensional gas-dynamic model with independent time discretization," *Proceedings of the ASME Internal Combustion Engine Division 2008 Spring Technical Conference*, 2008.

[12] J. Serrano, H. Climent, C. Guardiola, and P. P, "Methodology for characterisation and simulation of turbocharged diesel engines combustion during transient operation. part 2: Phenomenological combustion simulation," *Applied Thermal Engineering*, vol. 29, pp. 150–158, 2009.

[13] J. Luján, J. Galindo, J. Serrano, and P. B, "A methodology to identify the intake charge cylinder-to-cylinder distribution in turbocharged direct injection diesel engines," *Meas. Sci. Technol.*, vol. 19, p. 065401, 2008.

[14] C.-J. Chiang, A. Stefanopoulou, and M. Jankovic, "Nonlinear observer-based control of load transitions in homogeneous charge compression ignition engines," *IEEE Trans. on Cont. Sist. Technol.*, vol. 15, p. 438448, 2007.

[15] E. Bristol, "New measure of interaction for multivariable process control," *IEEE Transactions on Automatic Control*, vol. 11, pp. 133–134, 1965.

[16] L. del Re, L. Glielmo, C. Guardiola, and I. Kolmanovsky, "(eds.) automotive model predictive control: Models, methods and applications," *Lecture Notes in Control and Information Sciences*, vol. 402, 2010.

José Manuel Luján received the MS and PhD in Mechanical Engineering from the Universidad Politécnica de Valencia (Spain) in 1993 and 1998 respectively. He is Professor of Thermodynamics and Thermal Engines, and he develops his research in the CMT-Motores Térmicos of the Universidad Politécnica de Valencia. Prof. Luján leads research in air management and exhaust gas recirculation strategies of turbocharged internal combustion engines.

Carlos Guardiola received the MS in Mechanical Engineering from the Universidad Politécnica de Valencia (Spain) in 2000, and was honoured with the First National Award by the Spanish Education Ministry. He received the PhD degree in 2005 at the same university. In 1998 he started his research activity at the CMT-Motores Térmicos of the same university, where he serves now as Associate Professor. He leads research on control and diagnosis of internal combustion engines. He was co-editor of *Automotive Model Predictive Control: Model, Methods and Applications*.

Benjamín Pla started PhD studies at CMT-Motores Térmicos of the Universidad Politécnica de Valencia in 2004, after obtaining the MS in Mechanical Engineering from the same university. In 2008 he become Assistant Professor of Thermodynamics and Thermal Engines at the Universidad Politécnica de Valencia. A year later (2009) he received the PhD degree. His research is focused on the air management, turbo-charging and exhaust gas recirculation in diesel engines.

Pedro Cabrera López received the MS in Mechanical Engineering from the Universidad Politécnica de Valencia (Spain) in 2005. In 2008 he joined the CMT-Motores Térmicos of the same university and started his research activity, and is develops his studies for obtaining a PhD degree. His research interests include air management and control strategies.

ANEXO 2

NO_x closed-loop control in a turbocharged diesel engine through injection and air path coordinated model-based control

C. Guardiola, B. Pla, P. Cabrera

CMT Motores Térmicos, Universidad Politécnica de Valencia, Camino de Vera s/n, E-46022 Valencia, Spain

C. Carrión

ITACA, Universidad Politécnica de Valencia, Camino de Vera s/n, E-46022 Valencia, Spain

Abstract

In current automotive diesel engines exhaust gas recirculation is usually used for the control of the NOx production, and injection settings are optimised for the steady operation of the engine based on a multi-objective optimisation. Hence, during engine transients, where due to the slow turbocharger dynamics air charge composition can not be guaranteed, the selection of the injection settings is not optimal. However, since injection control can be performed in a cycle-to-cycle basis, and injected fuel quantity and timing can be closely controlled, the coordinated control of the air and fuel can be used for correcting the effect of the slow air path dynamics.

The focus of this paper is to describe a method for compensating the NO_x variation due to transients in the air path by means of a fast actuation on the start of the injection. Additionally, since NOx sensors have been recently been available in production engines, closed loop control of the NOx emission is demonstrated (while open loop solutions are also studied). For this objective, model predictive control techniques have been used; engine models were calculated using EGR valve and start of injection as system inputs, and NOx concentration and air mass flow as system outputs. The methods have been developed and validated through experimental tests on a turbocharged diesel engine.

Keywords: combustion engine; diesel engine; NOx; model predictive control; exhaust gas recirculation; start of injection; combustion control
PACS: 5.70.a, 89.40.Bb

1. Introduction

Nitrogen oxides (NO_x) emission abatement has been a hot research topic in diesel engines. Current technologies include exhaust gas recirculation (EGR) and, in recent years, catalytic after-treatment devices. EGR has become a generalised strategy for limiting the raw NO_x production; it consists in recirculating a certain amount of the exhaust gases in order to lower the combustion temperature, and hence NO_x formation[1]. EGR system is strongly coupled with the turbocharging system, what complicates EGR and boost control; as a consequence, it has been deeply studied in the past[9, 10].

On the other hand, injection control in diesel engines is usually treated as completely decoupled system, that is, injection settings are used independently of the ability of the boosting and EGR control system for ensuring the in-cylinder trapped air mass and composition. The exception to this are the 'smoke control' strategies, which limit the total fuel amount to be injected in order to do not surpass a given fuel-to-air ratio. Although this approach has been successfully used for years, new combustion techniques with higher sensibility to the in-cylinder conditions[2] or the

Stroke (S)	96 mm
Bore (D)	85 mm
S/D	1.129
Number of cylinders (z)	4
Displacement	2179 cm^3
Turbocharging system	Sequential parallel[5]
Valves by cylinder	4
Maximum power	125 $kW@4000\,rpm$
Compression ratio	17:1

Table 1: Engine main characteristics.

evolution of the emission regulations to more stringent standards will probably need of a joint control of the injection and air-path system.

The main advantage of a coordinated control can be obtained during air path transients: turbocharger dynamics (i.e. turbo-lag[3]) and emptying-and-filling processes in the manifolds[4] cause the air path control to be slow (in the scale of hundreds of milliseconds to several seconds). Hence, whenever a transient occurs, air mass flow and intake gas composition set-points cannot be perfectly tracked. As injection control can be performed in a cycle-to-cycle basis, because start of injection (SOI) and injected fuel amount can be closely controlled, the coordinated control can be used for correcting the effect of the error in the air path control.

Alternatively, improvements in the system control can be also found by means of the introduction of new sensors that directly measure the output quantities. In the last decade NO_x sensors have been developed and marketed[17, 18, 19], with their main application field for the control of after-treatment catalytic systems. Although these sensors are assumed to be slow[8] for control purposes, if installed at the turbine outlet such sensors could be used for the closed loop control of the raw NO_x production. For compensating the significant delays in the system a model based approach is proposed.

Model predictive control (MPC) controller is based on the availability of a mathematical system model, which is used for predicting the future system response and so taking decisions about the optimal system inputs (control actions) for tracking desired set-points. Different implementations have been proposed in the literature[15], varying in terms of the model used (linear or nonlinear, both of them with a wide variety of representations) and the possibility of dealing with restrictions (in the input signals, output signals, or internal states). Simplest cases admit explicit solutions, while numerical solvers are needed for the complex general cases. Hence calculation time becomes an issue when dealing with fast systems as the internal combustion engine is. In the past, MPC has been successfully used for the control of different subsystems of the internal combustion engine[15].

Present paper explores the possibilities of the MPC control of the EGR and the SOI for tracking the references in the air-path and NO_x emissions. This is done considering that a NO_x sensor may be available, but also an open loop compensation of the NO_x production during air-path transients will be tested. This last scenario could be easily applied to current series engines, since no additional sensors are used.

The paper is organised as follow: in Section 2 the experimental set-up is presented, including a description of the engine, the sensors and the system used for implementation of the controller; Section 3 is devoted to the model identification process, while the experimental results are presented and discussed in Section 4. Finally conclusions and future application ideas are presented in Section 5.

2. Experimental set-up

Test engine was an automotive 2.2-litre 4-cylinder common rail diesel engine. Engine specifications are shown in Table 1; for the experiments, all after-treatment devices were removed, since only raw emissions were monitored. The engine was installed on an engine test bench and coupled to a variable frequency eddy current dynamometer that allowed carrying out dynamical tests. In Figure 1 the layout of the experimental set-up is shown.

Original engine electronic control unit (ECU) implements a cascade control for the EGR system: a low level PID control strategy is used for tracking EGR valve position, which is imposed by a high level PID used for controlling

the intake air mass flow ($\dot{m}_a$). Air mass flow closed loop control is used for indirectly controlling NO_x output, since the lower level of $\dot{m}_a$ is obtained, the higher EGR rate is performed. The low level position controller is able to cope with the hysteresis and saturation effects, and it was profited in the present work; hence the control action for the MPC controller was the EGR valve position reference (u_{egr}).

For externally modifying the EGR valve set-point position a commercial bypass system (ETAS 910 which accessed the ECU through an ETK port, and Intecrio software) was used. Bypass also granted access to the SOI value u_{soi}, while several measured and calculated signals (including air mass flow value) were sent from the ECU to the external system via a CAN bus.

A Siemens VDO NO_x probe was installed at the turbine outlet; the sensor sent the NO_x concentration via CAN. The sensor was calibrated using a Horiba MEXA 7100D gas analyser as reference. Torque was measured by a Shenck sensor and opacity by an AVL 439 opacimeter.

As sketched in Figure 1, all signals were integrated and the MPC was programmed on a real-time National Instruments PXI, running with LabVIEW 2009. The PXI core was a 8170 RT controller with an Intel Pentium III processor running at 750 MHz, 500 MB RAM memory and 250 GB Hard disk memory. CAN card was used for communicating with the ETAS 910 and integrating NO_x signal, while analogical inputs were used for the rest of signals. All real-time routines (including MPC calculation) were scheduled with a 20 ms sampling time, which is generally used in many automotive applications.
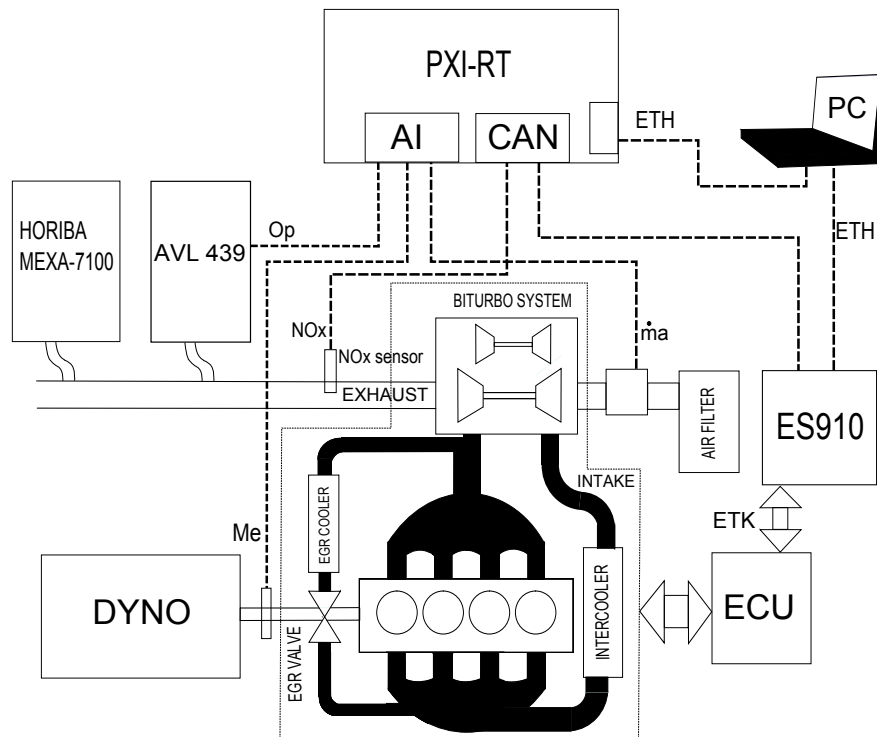

Figure 1: Experimental layout.

Selected engine nominal conditions for all tests shown in the paper are 1550 rpm and 60 Nm. At this operating point, nominal u_{soi} is -2.11 CAD (crank angle degrees) and nominal $\dot{m}_a$ is 64 kg/h, this last value roughly corresponds to a u_{egr} of 81% (since $\dot{m}_a$ is closed loop controlled, u_{egr} varies from test to test). Since the tests were run with constant injected fuel mass, slight variations in the torque were obtained and registered.

3. Model identification and MPC implementation

3.1. Model identification

MPC performance strongly depends on the model quality[15, 7], and hence lot of attention must be paid to the selection of the model structure and the identification process. For the present work, space state representation was selected, because solvers for the MPC implementation with these kind of models were available. The discrete state-space representation used was of the kind:

$$x_{t+1} = Ax_t + Bu_t$$
$$y_t = Cx_t + Du_t$$

(1)

where u_t is an array composed by stimulus signals (u_{egr} and u_{soi}), and y_t is an array that contains response signals (NO_x and $\dot{m}_a$). Multiple-input multiple-output (MIMO) model can be split into two multiple-input singe-output (MISO) models that can be identified through Gauss-Newton method on the basis of the evaluation of the prediction error on a given identification test[13].

Previously to the identification tests, the linearity of the system was checked. Figure 2 represents the steady state outputs of the system when varying u_{soi} while keeping nominal u_{egr} (left) and when varying u_{egr} with constant u_{soi} (right). Results are consistent with the expectations: u_{soi} has a nonlinear influence on NO_x, but does not affect $\dot{m}_a$, while u_{egr} presents a nonlinear effect on both $\dot{m}_a$ and NO_x. In addition to the nonlinearity in the input-output gain, the existence of saturations in the input quantities must be considered: u_{egr} must be kept within the range of the EGR valve (from full closed -100%- to full open -0%-); on the other hand, u_{soi} affects combustion and excessive in-cylinder peak pressure, noise and soot emissions must be monitored.
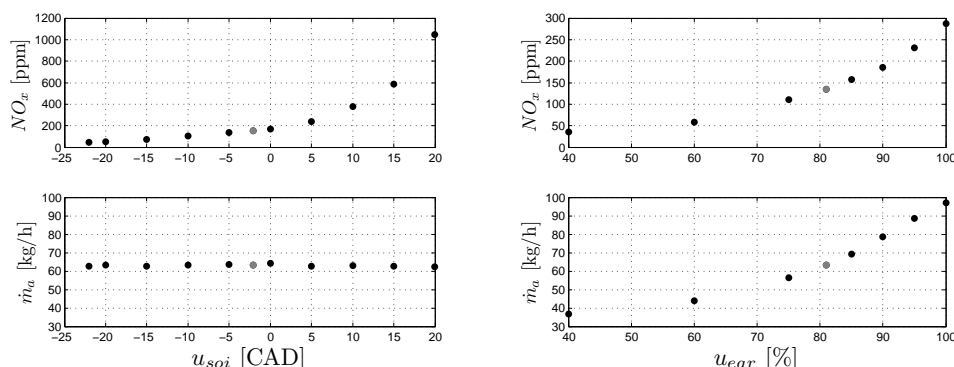

Figure 2: Effect of the variation of u_{soi} (keft) and u_{egr}. Positive values of u_{soi} correspond to advancing the main injection, represented in crank angle degrees [CAD]

Ortner and del Re[20] shows that the behaviour in the air-path system is significantly different when varying the EGR valve position, and suggests using different models (and MPC controllers) according to the valve position. This is done by means of a set of polytopes defined on the basis of engine load and speed, and EGR valve position. We adopt here this procedure, and since all tests are performed with constant engine load and speed, three operation zones of the EGR system are proposed, which correspond to u_{egr} values of 100%, 90% and 75%. These conditions are labelled as A, B and C respectively.

For identifying the system model, a set of experiments were done. They consisted on varying the system inputs (u_{egr} and u_{soi}) around their nominal value with a pseudo-random binary sequence (PRBS) profile. A characteristic example of the profile used in the identification tests is shown in Figure 3; for each operation condition A, B and C, three tests were done: constant u_{soi} and PRBS at u_{egr}; constant u_{egr} and PRBS at SOI; and u_{egr} and u_{soi} varying according to two independent PRBS.

Maximum and minimum levels of the PRBS profiles were selected according to Table 2 in order to mitigate the nonlinearity shown in Figure 2. In case of conditions A, the saturation of u_{egr} was considered.
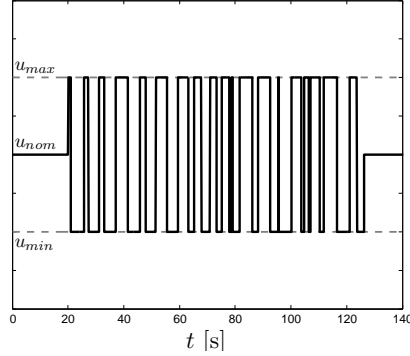
4

Figure 3: Example of PRBS used for the identification tests.

		A	B	C
$u_{egr,max}$	[%]	100	100	85
$u_{egr,nominal}$	[%]	100	90	75
$u_{egr,min}$	[%]	90	80	65
SOI_{max}	[CAD]	5.4	5.4	5.4
$SOI_{nominal}$	[CAD]	-2.1	-2.1	-2.1
SOI_{min}	[CAD]	-17.2	-17.2	-17.2

Table 2: PRBS signal values

For each one of the operating conditions, identification was done using a single test, while the other tests were used for validation. In the case of the model for NO_x, the test varying u_{soi} and u_{egr} was used for the identification process, while in the case of $\dot{m}_a$ the test with constant u_{soi} was selected for this purpose (since SOI does not significantly affects the air mass flow[8]). For both signals important delays were identified in the input-output response. Delays, which are summarised in Table 3, denote that the NO_x sensor response is very slow; such slow response is attributed to the sensor used[8]. The implications in the final control of the huge difference in the sensors dynamics will be discussed later in the paper.

Another implication of the delay in the NO_x sensor, is the necessity of correcting these delays beforehand: if this is not done the space state model would need a very high number of states in order to represent the system. If the delays are corrected by delaying the input the number of samples, the model can be reasonably represented with 4 state models, as shown in Figure 4. MISO models were identified for the air mass flow and NO_x for each of the operating conditions, then providing a set of matrices A, B, C and D valid for the local conditions. These matrices can be easily modified in order to represent the MISO system considering the non-delayed inputs. If d_1 and d_2 are the delays for input 1 and 2 respectively, $d_1 + d_2$ states must be added which act as memories for the inputs. This is easily done with the transformation shown in Figure 5, where the new set of matrices A', B', C' and D' are those for the non-delayed system. Finally, the MISO models independently identified for NO_x and $\dot{m}_a$ are aggregated into a single MIMO model.

Note that the approach used widely differs from directly identifying the non-delayed system: in the case of a 4 state

	NO_x	$\dot{m}_a$
u_{egr}	70	2
u_{soi}	43	-

Table 3: Input-to-output delay in samples, each of them corresponding to 20 ms.

5

model for NO_x, and considering the delays presented in Table 3, the total number of states would be $70 + 43 + 4 = 117$. Dimensions of A' would be then 117×117, which equals to 13689 coefficients to be identified (in opposition to the 16 coefficients of matrix A); this situation can cause non-singularities complicating the identification process and impacting on the model quality.
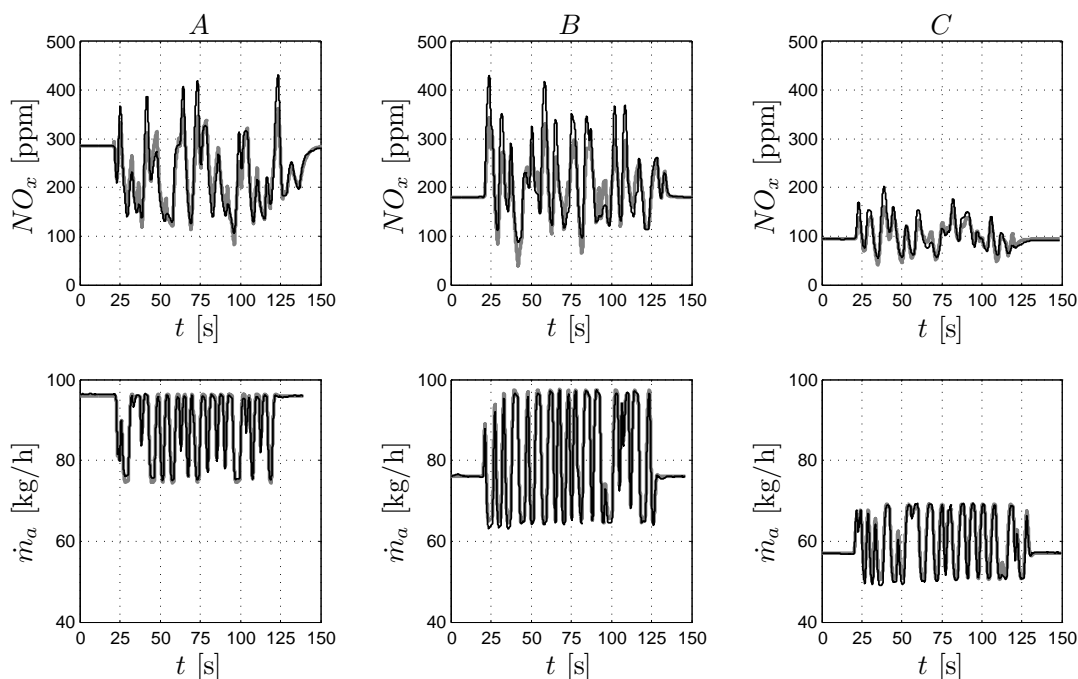

Figure 4: Identification results for the NO_x model (top) and $\dot{m}_a$ model (bottom). Modelled (gray) and measured (black) evolutions for the identification tests are shown.

Identification results for NO_x and $\dot{m}_a$ for conditions A, B and C are shown in Figure 4. Although a good agreement is obtained, several aspects can be highlighted:

- Note that the non-linearity of the system is still evident: positive peaks are different in gain to negative peaks. This can not be properly replicated by the linear space-state model because the linearisation proposed in Table 2 is not good enough. A Hammerstein-Wiener model could be used for coping this issue.

- Because of the precedent aspect, using a single linear model is not possible. Tables 4 and 5 show the relative mean absolute error (MAE) of using the identified model in each one of the tests, and demonstrates that the models are not interchangeable. However, when validating the model with a different test in the same conditions to those of identification the model behaves properly.

Hence, different models are used for conditions A, B and C, and consequently different MPC implementations are needed for each one of the conditions.

3.2. MPC implementation

MPC implementation used in the present work is based on a quadratic programming (QP) online solver, which is able to deal with space-state representation of the system. It computes the optimal set of control actions to be applied $u(k + i|k)$ in order to track the set-points according the following assumptions:

- The model behaviour is properly represented by the identified prediction model.
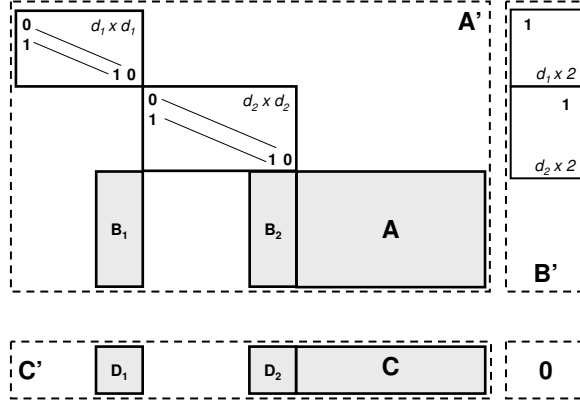
Figure 5: Block construction process for incorporating the delays d_1 and d_2 in an identified MISO model with 2 inputs. B_i corresponds to the i-th column of matrix B. Except those indicated, all elements in the matrices are equal to 0. Blocks dimensions marked in italics.

	A			B			C		
	u_{soi}	u_{egr}	both	u_{soi}	u_{egr}	both	u_{soi}	u_{egr}	both
model A	7.67	1.01	**5.64**	6.30	12.86	18.85	34.14	17.63	27.72
model B	7.81	40.44	59.00	5.37	3.77	**12.32**	31.51	138.78	121.11
model C	15.29	3.27	13.49	12.67	13.91	23.19	12.45	9.50	**8.55**

Table 4: Mean average error of the NO_x estimation (in %) when checking the identified models in different tests. Bold values refer to training tests for each model.

- There exists a cost function, being the optimal value of the future control actions that that minimises the cost function. Selected cost function for the present work is:

$$J(k) = \sum_{i=n_w}^{n_p+n_w} [\tilde{y}(k+i|k) - r(k+i|k)]^T * Q * [\tilde{y}(k+i|k)] + \\ \sum_{i=0}^{n_c-1} [\Delta u^T(k+i|k) * R * \Delta u(k+i|k)]$$

(2)

where $\tilde{y}(k+i|k)$ is the prediction in the system outputs, $r(k+i|k)$ is the desired trajectory, and $\Delta u(k+i|k)$ is the variation in the control actions; prediction horizon (from n_w to $n_w + n_p$ samples), control horizon (n_c, which equals the number of control actions to be computed) and cost weight matrices (Q and R) are the parameters of the controller.

- The control actions $u(k+i|k)$ (0% to 100% in u_{egr} and -17.2 CAD to 5.4 CAD in u_{soi}), and their rate of change $\Delta u(k+i|k)$, must be kept within the permissible range, and hence the problem becomes a restricted optimisation problem.

	A			B			C		
	u_{soi}	u_{egr}	both	u_{soi}	u_{egr}	both	u_{soi}	u_{egr}	both
model A	-	**0.56**	0.00	-	4.64	0.00	-	12.09	0.00
model B	-	23.05	0.00	-	**0.90**	0.00	-	7.82	0.00
model C	-	10.42	0.00	-	5.79	0.00	-	**1.45**	0.00

Table 5: Mean average error of the $\dot{m}_a$ estimation (in %) when checking the identified models in different tests. Bold values refer to training tests for each model.

The problem is solved for each time step (20 ms), and the optimal set of control actions for the next time step $u(k + 1|k)$ is applied; then the process is iterated again. MPC controller is able to deal naturally with MIMO systems; in addition, their basic operating concepts are easy to understand, and control adjustment in a engine is simple and intuitive, while allowing a proper consideration of saturation in the actuators. These are advantageous factors from the use perspective in practical applications, and hence MPC was used for the present work.

A commercial QP solver was used and the problem was solved using $n_p = 43$, $n_w = 107$ and $n_c = 2$. Cost weights Q and R were tuned for each operating condition. Although the MPC formulation allows using *a priori* known reference trajectory, future set-points are not usually known in automotive engines (because driving conditions are not easily and safely predicted), and hence $r(k + i|k)$ is considered equal to $r(k)$ in (2).

4. Results and discussion

Once MPC controllers were available for each condition, several tests were done for evaluating the capacity of using a coordinated control of the EGR system and of the SOI for the closed loop control of the NO_x exhaust concentration. Underlying idea was checking the capacity of the controller to reject the effect on NO_x emissions of the errors on the air-path control. Hence a simple check was done varying the air mass flow control reference (in steps of 10% and 20%).

Left plots in Figures 6 and 7 show the effect of a variation of the EGR control in operating conditions A and B (C has been omitted because results are similar to those in B) when the EGR control action is varied while keeping constant SOI. This situation is similar to the current control solution in automotive engines in the cases when control error occurs in the air-path control (for example, during transients): since u_{soi} is not adapted to the real manifold conditions, significant variations in NO_x emissions and opacity result.

Right plots in Figures 6 and 7 show equivalent plots to left plots but with the MPC controller. With regards to the original situation, here SOI is adapted in order to mitigate the effect of the variation in the air mass flow on the NO_x emissions. With regards to the initial situation, the system is able to compensate small variations in $\dot{m}_a$ (first two steps) and constant NO_x reference is maintained. That implies that SOI is advanced (positive value of CAD) when $\dot{m}_a$ is diminished: higher EGR rate would lower NO_x production, and hence advancing the injection is permissible. This also slightly improves engine torque and lowers opacity.

For higher values in the EGR rate, which corresponds to lower $\dot{m}_a$ reference (from 38 to 53 s in Figure 6, and from 45 to 55 s in Figure7) the saturation in u_{soi} is attained. In this case the high EGR rate causes NO_x to be below its reference, and SOI must be advanced for compensating it. The saturation in u_{soi} was set because excessively advancing the injection can increase engine noise [11], and excessive advancing of SOI can also lower the engine torque. In this case, the saturation in u_{soi} does not permit simultaneously tracking $\dot{m}_a$ and NO_x references and, on the basis of the selected weights in Q matrix, NO_x tracking is prioritised with regards to $\dot{m}_a$. Hence in these parts of the test the air mass flow set-point is not properly tracked.

On the other hand, if $\dot{m}_a$ is increased with regards to the nominal conditions (first step in Figure 7), which is equivalent to lowering the EGR rate, injection must be delayed in order to track the NO_x reference. Because of the magnitude of the step tested, significant variation in u_{soi} must be applied for tracking NO_x reference, and the delayed combustion affects negatively the engine torque. Although this impact on torque can be mitigated by means of increasing fuel injection in order to do not compromise driveability, the effect on the overall engine efficiency must be considered.

It may be argued that the presented method needs a NO_x sensor providing feedback of the raw NO_x emissions for the proper closed-loop control of this quantity. Using such sensor in series engines would impact engine cost and, while tailpipe sensors are foreseen for catalyst control and diagnostics[6], it is at least doubtful that emission sensors before any after-treatment devices will be included in marketed engines. However, the previous approach can be profited for performing a feed-forward correction of the SOI in order to mitigate the effect of the variation in $\dot{m}_a$.

Results show that even when the NO_x reference is not perfectly tracked, since no feedback on the measurement exists, a reasonably mitigation of the effect of varying $\dot{m}_a$ is obtained, due to the feed-forward action on u_{soi}. Hence, it is possible to extend the model-based approach for compensating the effect of the EGR control error when no NO_x sensor is available, and the model identification routines presented in the present paper are still valid.
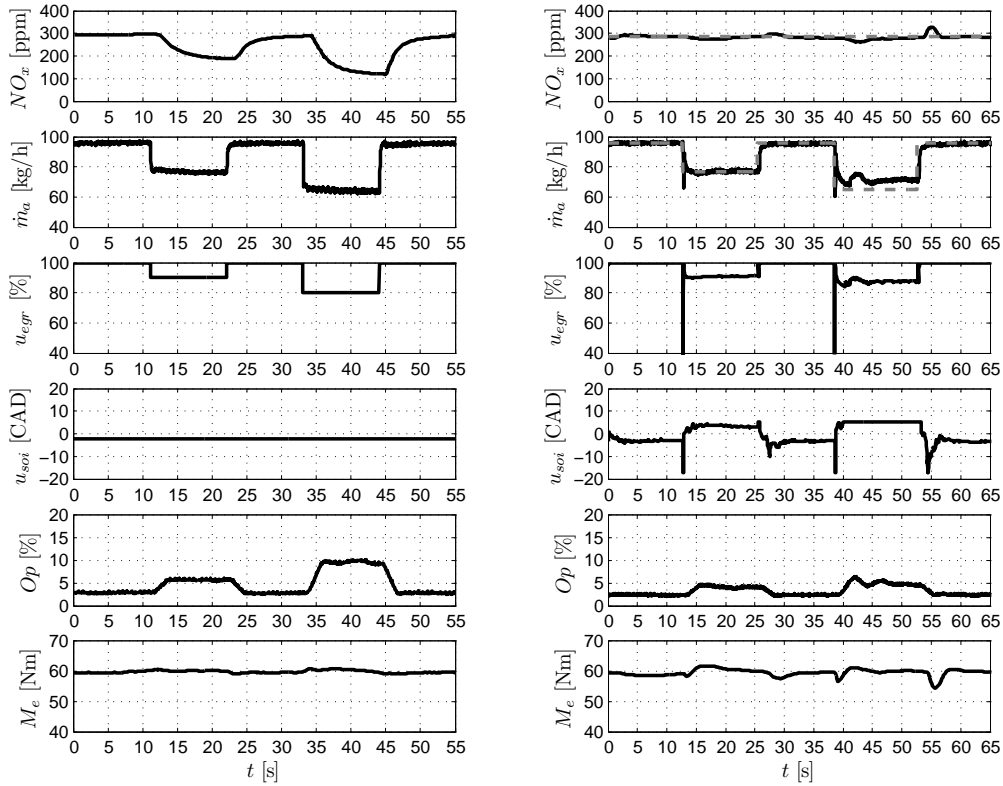
Figure 6: Results of the tests at operating conditions A. Left: open loop response of the engine to variations in u_{egr}. Right: closed loop MPC.

5. Conclusions

The paper has shown an implementation of a closed-loop control of the NO_x. The control is based on a MIMO controller, which simultaneously controls air mass flow and NO_x concentration actuating on EGR valve position and start of injection. Such approach, in opposition to the classical decoupled control of the air-path and combustion used in today's diesel engines, is able to track nominal NO_x output.

The effect of shifting SOI for compensating the $\dot{m}_a$ effect on NO_x can affect significantly engine torque, and modifications in the injected fuel mass (or alternatively limiting the SOI range) is proposed.

The proposed approach also permits deriving a feed-forward correction in SOI for the compensation of the EGR control system even when no NO_x sensor is available. However, the precision of this correction is strongly dependant on the model quality since no feedback exists.
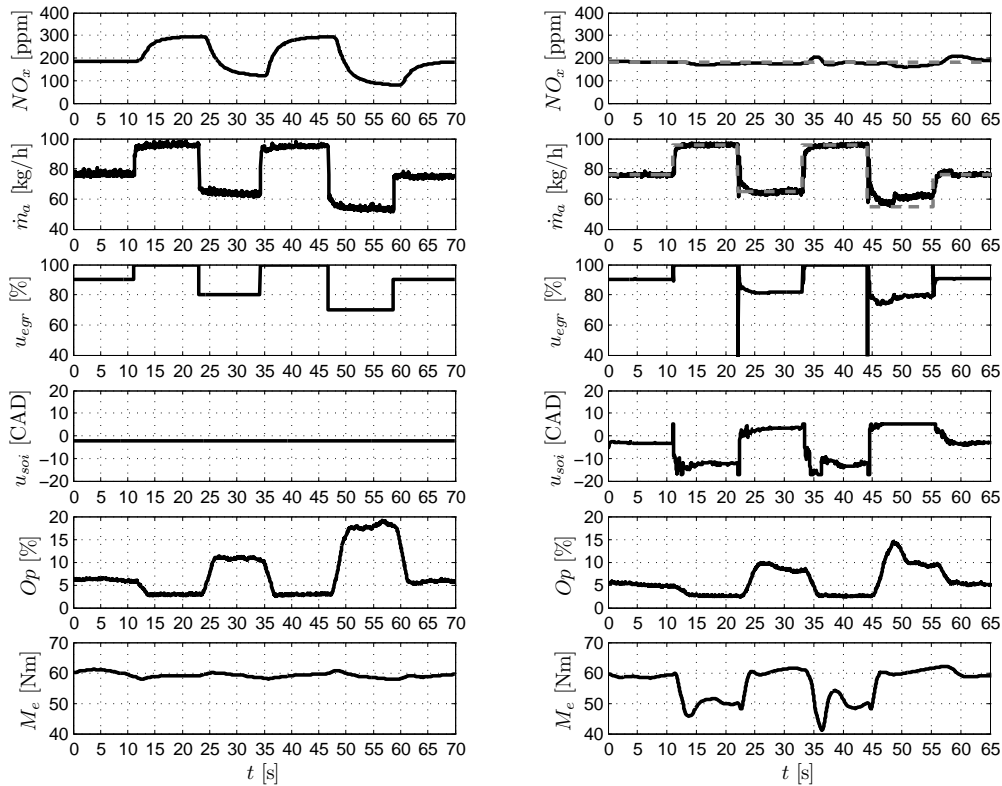
Figure 7: Results of the tests at operating conditions B. Left: open loop response of the engine to variations in u_{egr}. Right: closed loop MPC.

References

[1] Arregle, J., López, JJ., Guardiola, C. & Monin, C. (2010). On Board NOx Prediction in Diesel Engines: A Physical Approach. *Automotive Model Predictive Control: Models, Methods and Applications, Del Re L et al. (Eds)* ISBN-1849960704, Springer.

[2] Chiang, C.-J., Stefanopoulou, A.G. & Jankovic, M. (2007). Nonlinear Observer-Based Control of Load Transitions in Homogeneous Charge Compression Ignition Engines. *IEEE Trans. on Cont. Sist. Technol.*, vol. 15, pp. 438–448.

[3] Galindo, J., Climent, H., Guardiola, C. & Domenech, J.(2009). Strategies for improving the mode transition in a sequential parallel turbocharged automotive diesel engine. *International Journal of Automotive Technology*, Vol. 10, No. 2, pp. 141-149 .

[4] Serrano, J.R. , Climent, H. , Guardiola, C. & Piqueras, P.(2009). Methodology for characterisation and simulation of turbocharged Diesel engines combustion during transient operation. Part 2: Phenomenological combustion simulation. *Applied Thermal Engineering* Volume 29, Issue 1, Pages 150-158.

[5] Galindo, J. , Climent, H. ,Guardiola, C. & Tiseira, A.(2009). Assessment of a sequentially turbocharged diesel engine on real-life driving cycles.*International Journal of Vehicle Design* Volume 49, Number 1-3 / Pages: 214 - 234.

[6] Timothy, V. & Johnson. (2006). Diesel Emission Control in Review. *SAE paper 2006-01-0030*.

[7] Iwadare, M.,Ueno, M. & Adachi, S. (2009). Multi-Variable Air-Path Management for a Clean Diesel Engine Using Model Predictive Control. *SAE paper 2009-01-0733*.

[8] Galindo,J., Serrano,J.R., Guardiola,C. & Blanco-Rodriguez,D. (2010). An on-engine method for dynamic characterisation of a NOx concentration sensor. Submitted to *Experimental Thermal and Fluid Science*.

[9] van Nieuwstadt,M., Kolmanovsky,I., Moraal,P., Stefanopoulou,A. & Jankovic,M. (2000). Egr-vgt control schemes: Experimental comparison for a high-speed diesel engine, *IEEE Control Systems Magazine*, vol. 20, pp. 63–79.

[10] Stefanopoulou, A., Kolmanovsky, I., & Freudenberg,J.(2000). Control of variable geometry turbocharged diesel engines for reduced emissions, *IEEE Trans. on Cont. Sist. Technol.*, vol. 8, pp. 733–745.

[11] Heywood, J. (1988). Internal Combustion Engine Fundamentals *MacGraw-Hill*.

[12] Luján, JM., Galindo, J., Serrano, JR. & Pla, B. (2008). A methodology to identify the intake charge cylinder-to-cylinder distribution in turbocharged direct injection Diesel engines. *Meas. Sci. Technol.* **19** 065401.

[13] García-Nieto, S.,Martínez, M., Blasco, X. & Sanchis, J. (2004). Nonlinear predictive control based on local model networks for air management in diesel engines. *Control Engineering Practice.*

[14] Bermúdez, V., Luján, JM., Serrano, JR. & Pla, B. (2008). Transient particle emission measurement with optical techniques. *Meas. Sci. Technol.* **19** 065404.

[15] Del Re, L., Glielmo, L., Guardiola, C. & Kolmanovsky, I. (2010). Automotive Model Predictive Control: Models, Methods and Applications Series: Lecture Notes in Control and Information Sciences, Vol. 402 (Eds.) 1st Edition., 2010, VIII, 312 p. 152 illus., Softcover ISBN: 978-1-84996-070-0.

[16] Ogata, K. (2001). Modern Control Engineering (4th Edition), *Prentice Hall*.

[17] Kato, N., Nakagaki, K. & Ina, N. (1996).Thick Film ZrO2 NOx Sensor. *SAE paper 960334*

[18] Moos, R. (2005). A Brief Overview on Automotive Exhaust Gas Sensors Based on Electroceramics. *Int. J. Appl. Ceram. Technol.*, 2, 401-413.

[19] Riegel, J., Neumann, H., & Wiedenmann, H-M. (2002). Exhaust gas sensors for automotive emission control. *Solid State Ionics* 152-153, 783-800.

[20] Ortner, P. & del Re, L. (2007). Predictive Control of a Diesel Engine Air Path, *IEEE Trans. on Cont. Syst. Technol.* 15, 449-456.